Cement and Concrete Research 42 (2012) 467–475

Contents lists available at SciVerse ScienceDirect

Cement and Concrete Research

journal homepage: http://ees.elsevier.com/CEMCON/default.asp

The effect of SCMs on the corrosion of rebar embedded in mortars subjected to an acetic acid attack

O. Oueslati, J. Duchesne *

Centre de Recherche sur les Infrastructures en Béton (CRIB), Université Laval, 1065 ave de la Médecine, Québec, QC, G1V 0A6, Canada

ARTICLE INFO

Article history:
Received 23 May 2011
Accepted 19 November 2011

Keywords:
Organic acids (D)
Mortar (E)
SCMs
Reinforcement (D)
Corrosion (C)

ABSTRACT

Agricultural effluents are transformed under bacteria effect into organic acids which constitute severe chemical and electrochemical attacks for the reinforced concrete of agricultural structures. Among supplementary cementing materials (SCMs), blast-furnace slag (GBFS) and metakaolin (MK) are classified chemically resistant to the aggressiveness of acidic media and especially organic acids. The objective of this research was to evaluate the effect of GBFS and MK on the corrosion performance of reinforced mortars. Here, electrochemical measurements allow determining the time needed to initiate the corrosion. Mortar cylinders were made with three cement types including ordinary Portland cement (OPC), GBFS and MK cements at a fixed water/cementitious material (w/cm) ratio of 0.65. Corrosion of rebars was simulated by subjecting cylinder specimens to cyclic loading with acetic acid solution (pH 4, 0.5 M) and drying. Concrete resistivity and reinforcing steel potentials were measured up to 429 days of age. At the end of the experiment, all specimens were saw cut split open, and visually inspected. It was found that the drop in the linear polarization resistance and corrosion potential curves reflect the time needed to initiate the corrosion. Blending the cement with 20% of MK is beneficial with regard to delaying the onset of the corrosion by a factor of more than two. However, using high percentage of GBFS (80%) decreases the time to initiate the corrosion for specimen subjected to acetic acid attack.

1. Introduction

Intensification of farming practice is at the origin of environmental problems directly linked to the excess of effluents such as liquid manure and ensilage effluent [1]. Although animal excrement recycling was recognized as a practice that maintains and improves the fertility of soils [2], current policies aim for storage in water-tight silos, often built in concrete.

However, temporary storage of effluents produces many chemicals identified as having a detrimental effect on concrete and the reinforcing steel embedded in it. The agricultural effluents are quickly transformed under the effect of bacteria into organic compounds, in various quantities, among which are lactic acid and the volatile fatty acids (VFAs), such as acetic, propionic, butyric, iso-butyric and valeric acids. According to De Belie et al. [3], the acetic acid originates from the manure while the lactic acid is from acidified meal/water mixtures. The most aggressive acids seem to be those that produce easily soluble calcium salts, such as acetic acid [4–6]. According to Bertron [1], an acetic acid solution of pH 4 mimes well the aggressiveness of organic acids of liquid manure.

Agricultural effluents constitute a severe chemical threat toward the concrete of agricultural structures. In contact with an acetic acid solution, concrete will undergo an acido-basic reaction leading to the formation of soluble to very soluble salts in water [7–11]. In an immersion situation, those actions on concrete lead to the leaching of hydrates [12,13] causing premature corrosion of reinforcement steel [14–16] and degradation of the concrete [17,18].

It is very important to improve the durability performance of concretes for utilization in some applications, such as agricultural structure subjected to several organic acids of liquid manure or silage effluents. The resistance of concrete to such attack is not only determined by its permeability, but also by its alkalinity and the chemical composition of the cement paste [19]. Previous studies focussed on the chemical and mechanical resistance of cement-based materials subjected to organic acids. In previous works, the authors had the opportunity to study a large spectrum of binders made with ordinary Portland cement (OPC), OPC blended with silica fume (SF)/low-calcium fly ash (FA)/ground granulated blast furnace slag (GBFS) and metakaolin (MK) used at different replacement percentages, which were immersed in an acetic acid solution at a pH of 4 to simulate effluents from the agricultural and agrofood industries. The results showed that OPC control pastes present a very severe alteration [13]. Addition of silica fume or class F fly ash did not show any improvement compared to the control sample [13,17,20–25]. MK and GBFS mixtures presented the best resistance [26]. Furthermore, the results showed a direct relationship between

* Corresponding author. Tel.: +1 418 656 2177.
E-mail addresses: olfa.oueslati.1@ulaval.ca (O. Oueslati), josee.duchesne@ggl.ulaval.ca (J. Duchesne).

0008-8846/$ – see front matter © 2011 Elsevier Ltd. All rights reserved.
doi:10.1016/j.cemconres.2011.11.013

the percentage of OPC replacement by MK (15 and 20%) or GBFS (60 and 80%) and the increase in the chemical resistance [26]. Thus, only binders containing respectively 20% MK and 80% GBFS were used in this study in order to evaluate the corrosion resistance of reinforcements.

It is well known that the principal cause of degradation of steel reinforced structures is corrosion damage to the rebar embedded in the concrete [27,28]. The pore solution of concrete tends to be alkaline, with pH values over 12.5 [29,30]. Under such alkaline conditions, reinforcing steel tends to passivate and display negligible corrosion rates [31–33]. In contact with an acidic environment, the gradual penetration of the aggressive agent may break the passive film and depassivate the reinforcing rebars. On the other hand, the substitution of ordinary portland cement with SCMs leads to densification of the mortar which should better resist the percolation of the aggressive solution. Nevertheless, the use of SCMs is also accompanied by a decrease of the pH of the pore solution that can affect the passive film coating on steel that protects it from corroding. In this study, very high SCM content was used to improve concrete durability subjected to acidic solution, so, it is important to evaluate the corrosion resistance of such cement-based materials which oppose the decrease of the pH conditions and the densification of the matrix. The purpose of this investigation was to determine the effect of the incorporation of high content of MK and GBFS for specimens subjected to acetic acid attack on the initiation and propagation time of reinforcement corrosion.

Corrosion of reinforcing steel in concrete is a complex process that depends on the materials used in the test, environmental conditions, specimen type and test parameters [34].

Electrochemical measurements are the most commonly used to locate the corrosion areas of the reinforcing steel bars [35] and provide good information on the passive film repair or the passive film breakdown [36]. The electrochemical measurements allow determining the time needed to initiate the reaction and to follow the propagation phase [27,28,37]. Here, an experimental investigation of the corrosion of reinforcing steel bars embedded in mortar cylinders containing SCMs was undertaken. Corrosion tests were conducted to mimic the best natural conditions of exposure of mortar specimens subjected to an acidic solution responsible of the reinforcing bars corrosion. The experimental set up was inspired by a modified version of the ASTM G109 [38]. This method is indented for use in evaluating the relative performance of various SCMs. Corrosion testing consisted of weekly wetting (with an acetic acid solution at a pH of 4) and drying cycles applied to reinforced mortar specimens. Multiple electrochemical measurements such as corrosion potential, macrocell current, and polarization resistance are taken on a regular basis, and corrosion initiation is indicated by a change in all measurements. Specimens are broken open at the end of the experiment, when all the tested specimens were corroded, in order to visually examine the bars for confirmation of the electrochemical results.

2. Experimental process

2.1. Materials

This study was conducted on three mortars types made with OPC, designated in American Standard as GU (General Use), blended with 80% of GBFS and with 20% of MK, respectively, as partial cement replacement by mass. The control sample is made only of OPC. The chemical composition of the binders is given in Table 1.

The immersion solution was composed of acetic acid (CH_3COOH), a weak organic acid, with a dissociation constant pKa of 4.76 at 25 °C. The concentration of the acetic acid was 0.5 M at a pH 4.

2.2. Specimen making and treatment

Mortar samples were made at a high water/cementitious material (w/cm) mass ratio of 0.65 in order to obtain corrosion data in a reasonable time frame. The binder content was 393 kg/m^3. A uniformly graded Ottawa silica sand, Accusand C-109 from Unimin Corporation, was used at a content of 1430 kg/m^3. No superplasticizer, water reducing or air-entraining admixture was added. The procedure for mortars making was performed according to ASTM C192/C192M [39]. For the control sample, the compressive strength of 20 MPa was determined according to the ASTM C109M [40].

The embedded reinforcing bars consist of black steel 16 mm in diameter, and 200 mm in length. The reinforcing bars were cut into sections, cleaned in xylene, the ends were prepared and placed horizontally in 187-mm height and 150-mm diameter cylindrical molds (Fig. 1).

Reinforced specimens were demolded 24 h after pouring and stored in a wet room at 23 °C and 100% RH. After 6 months of moist curing, specimens were cut at a height of 127 mm in order to allow 20 mm of mortar cover over the top reinforcing bar. A polyvinyl chloride ponding reservoir (75 mm high, 100 mm diameter) was fixed with a silicone caulk above the specimen in order to contain the aggressive solution. Mortar specimens were completely coated with epoxy (Sikafloor 381) all around. The ponding reservoirs were filled with an acetic acid solution on a weekly schedule consisting of 4 days wet and 3 days dry at a constant temperature of 22 °C for a period of 429 days. A 10-Ohm resistor was attached between the top and bottom bars so that electrical parameters could be measured. For each binder tested, five companion specimens were prepared and tested simultaneously.

2.3. Tests implemented

Reinforcement corrosion of the embedded steel was monitored by measuring the corrosion potentials, macrocell current, and polarization resistance at regular intervals, once per cycle at the end of the wet cycle until the corrosion was initiated in the specimens. Experiments were stopped after 429 days of testing, even if the corrosion was not initiated in two of the five MK specimens. At the completion of all wet-dry cycling, all specimens were saw cut split open, and visually inspected.

2.3.1. Corrosion potential measurements (E_{corr})

Corrosion potential measurements give an indication of the probability of the corrosion activity through the measurement of the potential difference between a standard portable reference electrode and the reinforcing steel [41,42]. Corrosion potential readings were determined in accordance with ASTM C876 [43].

The corrosion potentials (E_{corr}) was measured between the working electrode (WE) (reinforcing steel bar) and the reference electrode (RE) placed on the upper surface of the concrete (Fig. 2). E_{corr} readings were measured using a Potentiostat Solartron SI 1260 recorded with respect to a saturated calomel electrode (SCE — Hg/Hg_2Cl_2). The standard potential of the SCE was −0.242 V compared to that of the standard hydrogen electrode. According to this method if the

Table 1
Chemical composition of binders.

Binders	%%CaO	%SiO_2	%Fe_2O_3	%Al_2O_3	%MgO	%MnO	%K_2O	%Na_2O	%TiO_2	%SO_3
OPC	62.5	19.6	2.27	4.9	2.61	0.05	0.9	0.24	0.25	2.57
MK	0.03	51.65	0.68	44.7	0.08	–	0.34	0.08	0.12	–
GBFS	37.31	36.77	0.85	7.77	13.91	1.02	0.43	0.31	0.36	–

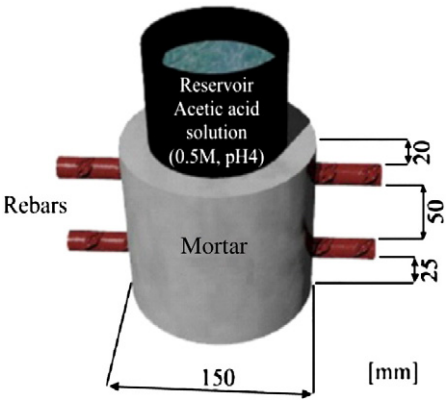

Fig. 1. Reinforced specimen configuration.

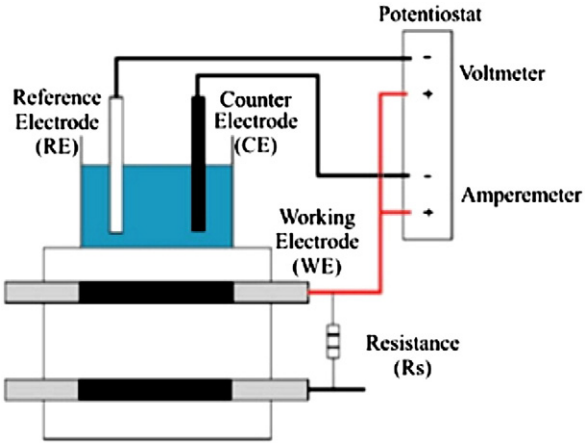

Fig. 3. Electrochemical measurements of linear polarization resistance.

potential of steel in concrete becomes more negative than −276 mV vs. SCE there is a 90% probability that corrosion will occur [44].

2.3.2. Linear polarization resistance measurements (Rp)

The polarization resistance, Rp, is the ratio of the applied potential to resulting current and is inversely proportional to the corrosion rate [45,46].

Polarization resistance measurements were determined in accordance with ASTM G59 [47]. The experimental setup (Fig. 3) requires three electrodes: the working electrode (WE), the reference electrode (RE) and the counter electrode (CE). A graphite CE was used.

The polarization technique consist to impose a potential or a current to an electrode and to measure the corresponding current or potential [48]. The counter electrode conducts the current to the working electrode in order to generate its polarization.

In this test method, a small potential scan, between −0.02 V and 0.02 V, is applied while maintaining the equilibrium between the two electrodes (CE and RE). The resultant currents, between the working electrode and the counter electrode are simultaneously recorded.

The reference electrode potential is always fixed. The working electrode potential is measured versus the reference electrode potential.

The recording system allows to follow the evolution of the polarization curve I = f (E). The polarization resistance Rp of a corroding electrode is determined by measuring the slope of the polarization curve over the range ±10 mV [49].

The slope represents the apparent resistance (Rapp) which is the sum of the resistance of concrete (R_Ω) and the polarization resistance (Rp). However, R_Ω is negligible [50].Thus, Rapp = Rp.

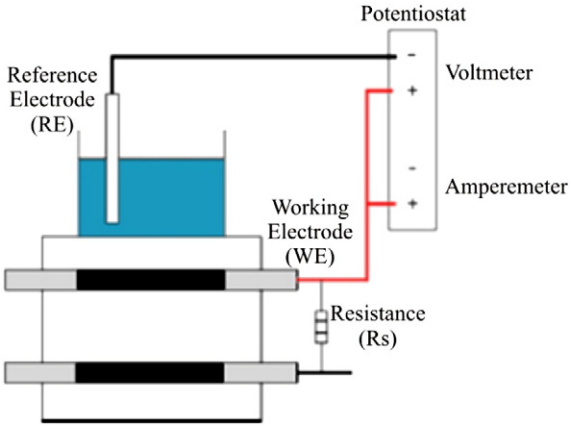

Fig. 2. Electrochemical measurement of the corrosion potential (E_{corr}).

The polarization resistance is usually expressed in $k\Omega \times cm^2$ in order to reflect the surface exposed to corrosion. The steel surface exposed is fixed to 51 cm^2.

The threshold for corrosion initiation was fixed at 5000 $\Omega \times cm^2$. A value of Rp higher than 5000 $\Omega \times cm^2$ indicates a state of no corrosion.

3. Results

3.1. General aspect of mortar specimens

Fig. 4 shows the appearance of OPC, MK and GBFS mortar samples at the end of the experiment i.e. after 429 days of cycles of wetting and drying using an acetic acid solution (pH 4, 0.5 M). The appearance of the acetic acid solution in contact with the OPC mortar (Fig. 4A) shows a major dissolution of the cement paste. In fact, many sand grains were detached from the mortar and accumulated in the reservoir (4B). Fig. 4C presents the acetic acid solution in contact with the MK samples. The solution is clearer resulting from a lower dissolution rate of MK specimens. This was confirmed by the surface of the specimen that is slightly degraded with a few sand grains visible in the reservoir (4D). Finally, Fig. 4E shows the acid solution in contact with the GBFS sample and the surface of that sample (4F). The solution is lighter with only slight degradation of the surface which confirms the good chemical resistance of the GBFS mortar against acetic acid attack [26].

3.2. Evolution of the corrosion potential measurements (E_{corr})

Fig. 5 presents the corrosion potential measured on reinforced mortars as a function of time. The horizontal blue lines show the threshold value corresponding to the corrosion probability criterion suggested in the ASTM C876 (potential of −276 mV with respect to a saturated calomel electrode [44]). Values more negative than −276 mV correspond to a 90% probability of corrosion. Corrosion initiation is shown in Fig. 6 by a drastic drop of the corrosion potential.

The corrosion was initiated between 165 and 185 days for the OPC samples exposed to the acetic acid solution (Fig. 5A). The corrosion potential dropped at only 89 days for one companion specimen. MK samples (Fig. 5B) present significant improvements in corrosion compared with OPC samples. The corrosion was initiated after 324 days of exposition and two companion samples out of five were not corroded at the end of the experiment (429 days). Fig. 5C presents the corrosion potential curves for the GBFS samples. The corrosion was initiated after only 21 days for the five companion specimens.

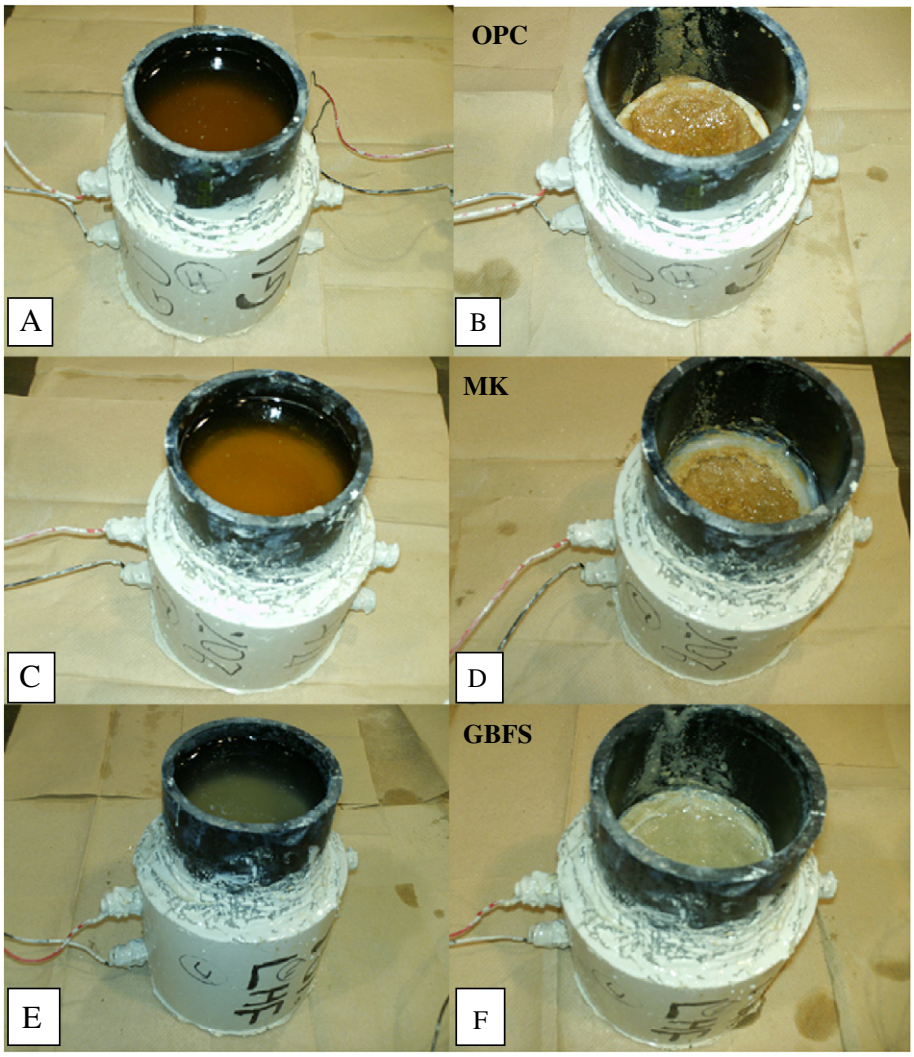

Fig. 4. Aspect of the acetic acid solution (A, C, E) and the surface of the specimen after 429 days of wetting/drying cycles (B, D, F) for OPC, MK, and GBFS respectively.

3.3. Evolution of the linear polarization measurement (Rp)

Fig. 6 presents the linear polarization resistance measurements as a function of time. The initiation of the corrosion was marked by a sudden drop in the polarization resistance curve. The threshold of the corrosion initiation was set at a value of $<5\ k\Omega \times cm^2$ presented by a blue line on the polarization resistance curves. This technique allows determining the time needed to initiate the reaction of corrosion and do not directly translate to the corrosion rates.

Fig. 6A shows that the corrosion was initiated between 184 and 198 days for the OPC samples exposed to the acetic acid solution. The linear polarization resistance dropped at only 64 days for one companion specimen. This same behavior was observed with the corrosion potential measurements. MK samples (Fig. 6B) present significant improvements in corrosion compared with OPC samples. The corrosion in the MK specimens was initiated between 338 and 352 days of exposition and two companion samples out of five were not corroded at the end of the experiment (429 days). Fig. 6C presents the polarization resistance curves for the GBFS samples. A drop in the polarization resistance was observed at the beginning of the test with a sudden drop more pronounced between only 23 to 26 days. Then, the linear polarization resistance continues to drop which indicates the initiation and the propagation of the corrosion. Corrosion products were seen at the surface of the GBFS specimens after only one month of wetting/drying cycles with the acetic acid (Fig. 7).

3.4. Aspect of the reinforcing bars at the end of the test

Fig.8 shows the distribution of the corrosion products on the reinforcing bars of OPC, MK and GBFS mortars. For the three samples, the top rebars of the specimens show some signs of pitting corrosion localized on the central part of the rebars at the interfaces steel/mortar. Under the top rebars, corrosion products are distributed all over the central part of the rebars. No corrosion product was observed next to the bottom bars of the OPC and MK samples. GBFS samples are the only one showing corrosion products close to the bottom rebars. The corrosion products are composed of adherent dense black rust for the OPC and GBFS samples while MK samples present non-adherent porous brown–red rust.

Reinforcing bars of OPC and GBFS mortars present important deterioration as seen in Fig. 9. The mass losses of GBFS reinforcing bars are the most important causing a loss of ductility.

4. Discussion

Reinforcing bars embedded in mortar are surrounded by an alkaline solution which produces rapid oxidation of the steel surface forming a passive film which protects the rebar [37]. However, the percolation of the acetic acid solution (pH4, 0.5 M) within the cement matrix lowers the pH of the pore solution around the reinforcing bars

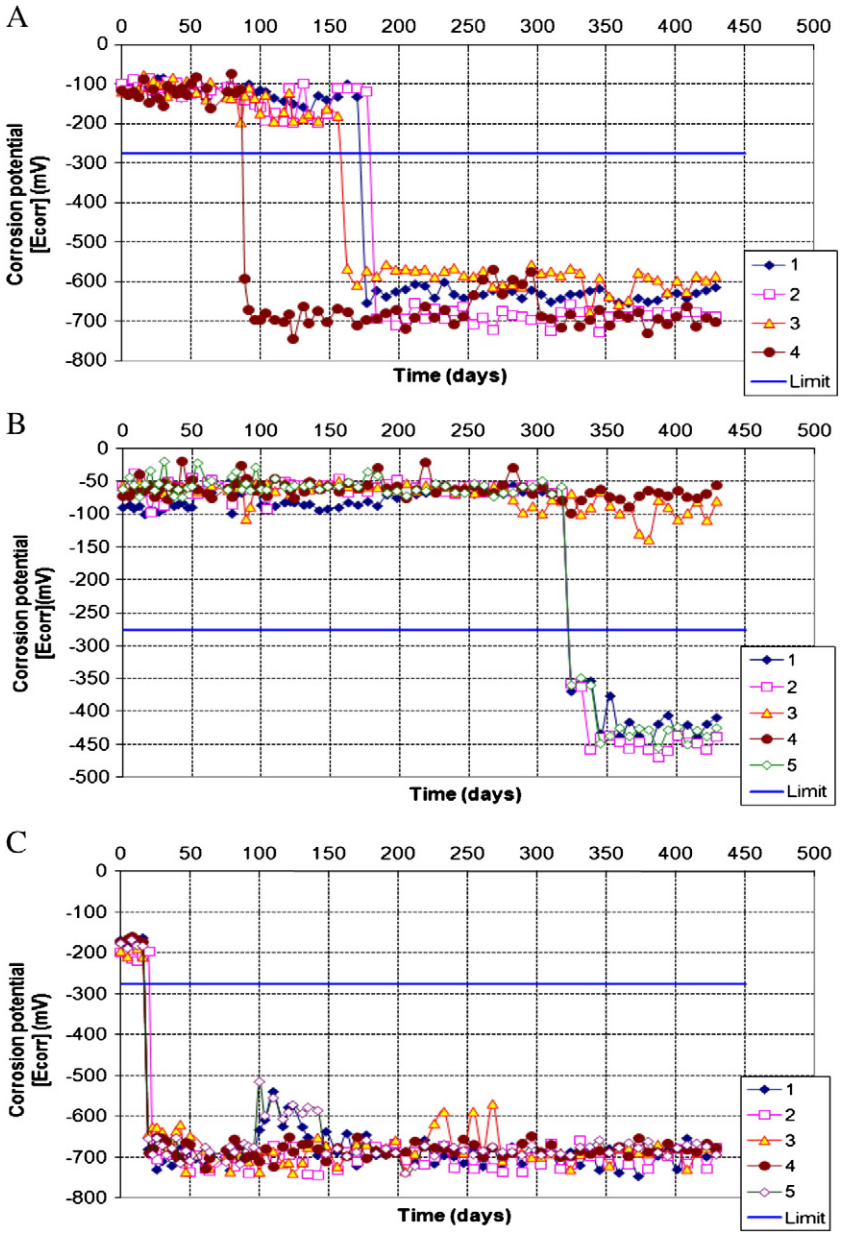

Fig. 5. Corrosion potential (E_{corr}) of reinforcing bars in mortars for the five companion specimens. A) OPC; B) MK; C) GBFS.

which favors the initiation of the corrosion. Corrosion reaction in presence of an acidic attack can be compared to that of the carbonation reaction which is mainly due to a decrease of the pH conditions around the rebars and to a destabilization of the passive film around them. The portlandite ($Ca(OH)_2$ or CH) produced by the hydration reaction helps prevent the corrosion of reinforcing steel by offering pH buffer to the pore solution. However, the portlandite may also be utilised to produce further C–S–H through the pozzolanic reaction with SCMs. A depletion of the portlandite content may result in a decrease in the pH of the pore solution. Both phenomenon, percolation of an acidic solution and depletion of the portlandite, may decrease the pH around the rebars and initiate the corrosion.

Some SCMs, like GBFS and MK, improve considerably the chemical and mechanical durability of concrete submitted to an acetic acid solution. According to Oueslati [26], GBFS and MK improve the chemical resistance of cement-based materials subjected to organic acid due to their chemical compositions which are rich in silicon, aluminum and iron, elements resistant in acidic environment, and low in calcium, the most leachable element in an acidic solution. In this study, the chemical resistance of the different specimens was evaluated by the appearance, mainly clearness, of the acetic acid solution in the ponding reservoirs and by the condition of the surfaces of the reinforced specimens. GBFS samples were the more chemically resistant to the acid attack, followed by MK samples.

4.1. Corrosion initiation time of reinforced mortar specimens

Electrochemical measurements, corrosion potential and linear polarization resistance, were monitored over time. The corrosion initiation time was indicated by a sudden drop in the electrochemical measurements. The average initiation time was 153, 21, and 324 days measured by the corrosion potential and 159, 25, and 345 days monitored by the polarization resistance on OPC, GBFS, and MK specimens, respectively. Moreover, average corrosion initiation time should be longer for MK specimens considering that two out of the five samples were not corroded at the end of the experiment, after 429 days. In all cases, results are

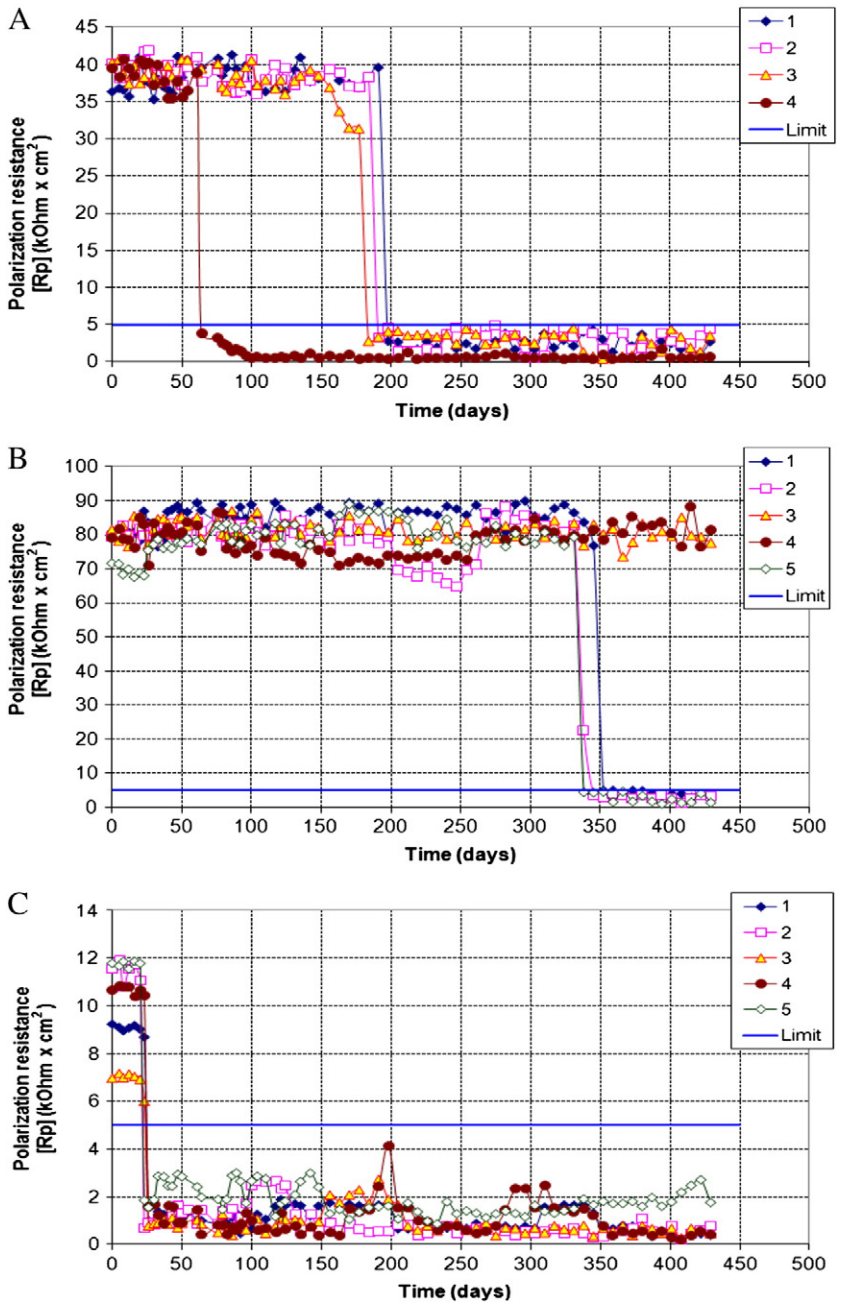

Fig. 6. Linear polarization resistance of reinforcing bars in mortars for the five companion specimens. A) OPC; B) MK; C) GBFS.

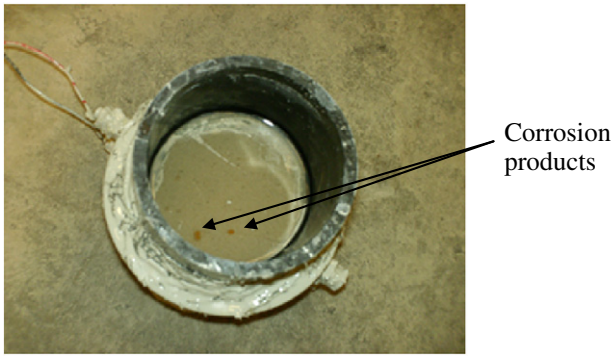

Fig. 7. Capillary rise of corrosion products on the surface of the GBFS mortar specimens after 1 month of wetting and drying cycles using an acetic acid solution (pH4, 0.5 M).

comparable between the two methods with longer initiation time measured with the polarization resistance method. These results showed that blending the cement with MK is beneficial with regard to delaying the onset of the corrosion by a factor of more than two. However, using high percentage of GBFS decreases the time to initiate the corrosion even if this sample demonstrated the best chemical performances against the acid attack. After one month of experiment, visual inspection of the GBFS reinforced specimen showed no trace of matrix dissolution (Fig. 4F), but corrosion products were seen at the surface of the specimens (Fig. 7). This indicates that there is no direct relationship between the corrosion and the chemical resistance of the specimens.

The corrosion initiation is related to the penetration of the acid solution within the cement matrix and it is directly connected to the transport properties of mortar specimens. The water/cementitious material (w/cm) ratio, the cement type and content are some factors among others that influence the corrosion initiation time, as they have a direct effect on the diffusion coefficient of the cement matrix [51,52]. In this

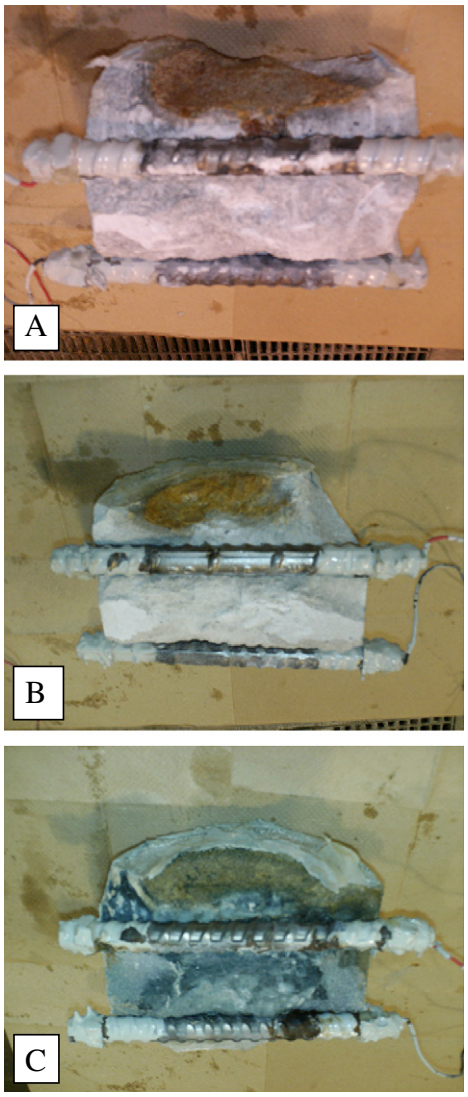

Fig. 8. Distribution of the corrosion products on the reinforcing bars of A) OPC B) MK and C) GBFS mortars after 429 days of wetting and drying cycles using an acetic acid solution (pH4, 0.5 M).

study, the high water/cementitious material (w/cm = 0.65) ratio used has the disadvantage to increase the transport properties of the blended mortars and GBFS (a latent hydraulic binder) specimens are by far more affected.

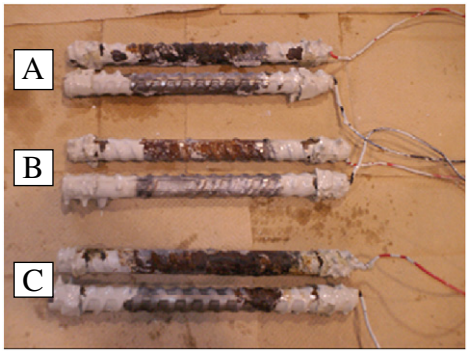

Fig. 9. Distribution of the corrosion products on the top and bottom reinforcing bars of A) OPC B) MK and C) GBFS mortars after 429 days of wetting and drying cycles using an acetic acid solution (pH4, 0.5 M).

The high porosity of the GBFS samples promotes percolation of the acid solution through the mortar specimens. In addition, the use of 80% of GBFS as cement replacement allows a slight decrease in the pH of the pore solution. The replacement by mass of OPC with GBFS involved a significant decrease in the amount of hydrated phases in particular C–S–H and portlandite [53,54]. Portlandite depletion in high GBFS sample is due to a very rapid dilution effect related to the fact that portlandite results from cement hydration, which in turn is directly related to the cement proportion in the mix and to the pozzolanic reaction between portlandite and SCM which is low for GBFS hydration [55]. Both the intrusion of acid solution through the mortar samples and the portlandite depletion due to high GBFS content may have contributed to a decrease in the pH conditions around the reinforcing bars and to the initiation of the corrosion.

On the other hand, the first part of this work [56] shows that, after 28 days of curing, MK addition allows an important decrease of the total volume of pores as well as a large contribution to the refinement of pores compared to control OPC samples. In fact, MK samples present only 26.6% of pores larger than 0.1 μm contrary to 40% for the OPC samples [24,56]. Thus, the low porosity and the high compactness of the MK specimens slowed down the acid solution percolation through the mortar cover and increased the corrosion initiation time. It is well-known that replacement of cement with metakaolin produces a general refinement of the pore structure [57]. According to Page [58], MK addition decreases substantially the pH of the pore solution with pH value of 12.9 measured on pore solution of cement paste made with 20% of MK cured for 80 days. In spite of this reduction of the pH, the pH conditions are alkaline enough to maintain the passive film around the reinforcing bars.

The corrosion propagation depends on the aggressiveness of the acid solution and the nature of corrosion products formed. For MK mortar specimens, the oxidation products consist on a non-adherent porous brown–red rust which is a superficial deterioration of the reinforcing bars easily flaked off with a razor blade. However, for the OPC and GBFS mortar specimens, the oxidation products present an extremely adherent compact and dense black rust characteristic of a more deeper degradation of the reinforcing bars [27,59].

5. Conclusion

This study presents an experimental investigation of the corrosion of reinforcing steel bars embedded in mortar cylinders containing SCMs. Corrosion tests were conducted to mimic the natural conditions of exposure of mortar specimens subjected to an acidic solution as found in agricultural structures. Corrosion testing consisted of weekly wetting (with an acetic acid solution at a pH of 4) and drying cycles applied to reinforced mortar specimens. Electrochemical measurements such as corrosion potential and linear polarization resistance were taken on a regular basis, and corrosion initiation was indicated by a drastic drop in all measurements. Specimens were broken open at the end of the experiment to visually examine the bars for confirmation of the electrochemical results. Results obtained show that:

- GBFS samples were the more chemically resistant to the acid attack, followed by MK samples and finally OPC samples. The chemical resistance was evaluated by the appearance, mainly clearness, of the acetic acid solution in the ponding reservoirs and by the condition of the surfaces of the reinforced specimens.
- Corrosion initiation time measured by the corrosion potential and linear polarization resistance methods were comparable with slightly longer initiation time measured by the latter method.
- Blending the cement with 20% of MK is beneficial with regard to delaying the onset of the corrosion by a factor of more than two compared to OPC specimens at a w/cm ratio of 0.65. However, using high percentage of GBFS (80%) decreases the time to initiate

the corrosion by a factor of about eight at a w/cm ratio of 0.65 for specimen subjected to acetic acid attack.

- Both phenomena, percolation of an acidic solution and depletion of the portlandite, may decrease the pH around the rebars and initiate the corrosion. The porosity of the material seems the main factor controlling the corrosion initiation time knowing that MK and GBFS are both chemically resistant to acidic attack.

Acknowledgments

This study has been supported by the National Science and Engineering Research Council of Canada (NSERC) and by the Fonds de recherche sur la nature et les technologies of the Province of Québec (FQRNT).

References

[1] A. Bertron, Durabilité des matériaux cimentaires soumis aux acides organiques. Cas particulier des effluents d'élevage, Thèse de Doctorat, INSA de Toulouse, France, 2004, 250 pp.
[2] J. Martinez, G. Le Bozec, Déjections porcines et problèmes environnementaux en Europe, Cah. Agric. 9 (2000) 181–190.
[3] N. De Belie, B. De Blaere, R. Verschoore, Compounds aggressive to concrete floors in pig houses, Landwards 51 (3) (1996) 22–26.
[4] I. Biczók, Concrete Corrosion, Protection of Concrete, Verlag der Ungarischen Akademie der Wissenschaften, Budapest, 1960.
[5] V.M. Moskvin, T.V. Rubetskaya, G.V. Ljubarskaya, Concrete corrosion in acidic media and methods for its investigation, Beton Zhelezobeton (Moscow) 10 (1971) 10–12.
[6] V.M. Moskvin, F.M. Ivanov, S.N. Alexejev, E.A. Gusejev, Corrosion of Concrete and Reinforced Concrete: Methods for their Proctection, Strojizdat, Moscow, 1980.
[7] A. Kleinlogel, The Influence of Different Physical Chemical Elements on Concrete, 1st Ed. Dunod, Paris, 1960.
[8] Lange, in: John A. Dean (Ed.), Lange's Handbook of Chemistry, 30th Edition, Mc Graw Hill Book Company, 1985.
[9] V. Zivica, A. Bajza, Acidic attack of cement based materials — a review. Part 1. Principle of acidic attack, Const. Build. Mater. 15 (2001) 331–340.
[10] D.R. Lide, Handbook of Chemistry and Physics, 72nd edition CRC Press, Inc., 1991–1992
[11] A. Bertron, J. Duchesne, G. Escadeillas, Accelerated tests of hardened cement pastes alteration by organic acids: analysis of the pH effect, Cem. Concr. Res. 35 (2005) 155–166.
[12] A. Bertron, M. Coutand, X. Cameleyre, G. Escadeillas, J. Duchesne, Attaques chimique et biologique des effluents agricoles et agroalimentaires sur les matériaux cimentaires, Mat. Tech. 93 (2005) 111–121.
[13] O. Oueslati, J. Duchesne, Acetic acid attack of blended cement pastes, in: M.G. Alexander, A. Bertron (Eds.), Concrete in Aggressive Aqueous Environments — Performance, Testing and Modelling, Toulouse 3–5 June 2009, Rilem publication S.A. R.L.PRO, 63, 2009, pp. 108–115.
[14] V. Assaad Abdelmseeh, J. Jofriet, G. Hayward, Sulphate and sulphide corrosion in livestock buildings, Part I: concrete deterioration, Biosyst. Eng. 99 (2008) 372–381.
[15] V. Assaad Abdelmseeh, J. Jofriet, G. Hayward, Sulphate and sulphide corrosion in livestock buildings, Part II: reinforcing steel corrosion, Biosyst.Eng. 99 (2008) 382–389.
[16] A.F. Idriss, Satish C. Negi, Jan C. Jofriet, Gordon L. Hayward, Corrosion of steel reinforcement in mortar specimens exposed to hydrogen sulphide, Part 1. Impressed voltage and electrochemical potential tests, J. Agric. Eng. Res. 79 (2) (2001) 223–230.
[17] A. Bertron, G. Escadeillas, J. Duchesne, Attack of cement pastes exposed to organic acids in manure, Cem. Concr. Compos. 27 (2005) 898–909.
[18] V. Zivica, Deterioration of cement-based materials due to the action of organic compunds, Constr. Build. Mater. 20 (2006) 634–641.
[19] N. De Belie, J.J. Lenehan, C.R. Braam, B. Svennerstedt, M. Richardson, B. Sonck, Durability of building materials and components in the agricultural environment. Part III: concrete structures, J. Agric. Eng. Res. 76 (2000) 3–16.
[20] V. Pavlík, Corrosion of hardened cement paste by acetic and nitric acids. Part III: influence of water/cement ratio, Cem Concr Res 26 (3) (1996) 475–490.
[21] J. Madrid, J.M. Diez, S. Goni, A. Macias, Durability of ordinary portland cement and ground granulated blast furnace slag cement in acid medium, Proceedings of 10th International Congress on the Chemistry of Cement, Gothenburg, Sweden, Vol. 4, 1997, p. 4iv040.
[22] D. Israel, D.E. Macphee, E.E. Lachovski, Acid attack on pore reduced cements, J. Mater. Sci. 32 (1997) 4109–4116.
[23] V. Pavlík, S. Uncík, The rate of corrosion of hardened cement pastes and mortars with additive of silica fume in acids, Cem. Concr. Res. 27 (11) (1997) 1731–1745 Erratum: Cem Concr Res 28 (6) (1998) 936–938.
[24] O. Oueslati, J. Duchesne, Acetic acid attack of cement matrix: evaluation of durability parameters, in: Á. Palomo, A. Zaragoza, J. Agüí (Eds.), Proceeding of the 13th International Congress on the Chemistry of Cement, Madrid, July 3–8, 2011, pp. 483–489.
[25] O. Oueslati, J. Duchesne, Impact of acetic acid attack on the chemical, physical and mineralogical evolution of cement pastes, in: S. Godbout (Ed.), Proceeding of the 7th International Symposium on Cement Based Materials for a Sustainable Agriculture (CSAS), Quebec City, Canada, September 18–21, 2011, pp. 28–39.
[26] O. Oueslati, Durabilité des matériaux cimentaires soumis aux acides organiques. Résistance chimique, mécanique et de corrosion, Thèse de Doctorat, Université Laval, Canada, 2011, 370 pp.
[27] F. Paradis, Influence de la fissuration du béton sur la corrosion des armatures - caractérisation des produits de corrosion formés dans le béton, Thèse de Doctorat, Université Laval, Canada, 2009, 171 pp.
[28] M.A.A. Tullmin, C.M. Hansson, P.R. Roberge, Electrochemical techniques for measuring reinforcing steel corrosion, technical sessions for InterCorr/96, session 1: industry focus session: assessment of corrosion of steel in concrete, http://64.224.111.143/events/intercorr/techsess/papers/session1/abstracts/tullmin.html.
[29] A.M. Neville, J.J. Brooks, Concrete Technology, Longman Scientific & Technical, UK, 1987.
[30] H.F.W. Taylor, Cement Chemistry, 2nd edition, 1997, Thomas Telford Publishing, London.
[31] A. Rosenberg, C.M. Hansson, C. Andrade, Mechanisms of corrosion of steel in concrete, Materials Science of Concrete 1, Am. Ceram. Soc. (1989) 285–314.
[32] J.P. Broomfield, Corrosion of Steel in Concrete — Understanding, Investigation and Repair, Publ. Taylor and Francis, London, 2007.
[33] A. Bentur, S. Diamond, N. Berke, Steel Corrosion in Concrete — Fundamentals and Civil Engineering Practice, E & FN Spon, 1999 201 pp.
[34] C.M. Hansson, A. Poursaee, S.J. Jaffer, Corrosion of Reinforcing Bars in Concrete, Portland Cement Association, 2007 PCA R&D Serial No. 3013.
[35] A. Raharinaivo, G. Grimaldi, C. Mierzejewski, Caractérisation de la corrosion des aciers dans le béton par des méthodes électrochimiques, Congrès COFREND, Reims, CND & Corrosion, Cédérom, 2001.
[36] K. Saker, Effect of cement type on the corrosion of reinforcing steel bars exposed to acidic media using electrochemical techniques, Cem. Concr. Res. 35 (2005) 1820–1826.
[37] V. Lapointe, Initiation et propagation de la corrosion dans un élément de béton armé, Mémoire de maîtrise, Université Laval, 2007 84 pp.
[38] ASTM G109, Standard Test Method for Determining the Effects of Chemical Admixtures on the Corrosion of Embedded Steel Reinforcement in Concrete Exposed to Chloride Environments, ASTM International, West Conshohocken PA, 1992.
[39] ASTM C192/C192M, Standard Practice for Making and Curing Concrete Test Specimens in the Laboratory, ASTM International, West Conshohocken PA, 2007.
[40] ASTM Standard C109/C109M, Standard Test Method for Compressive Strength of Hydraulic Cement Mortars (Using 2-in. or 50-mm Cube Specimens), ASTM International, West Conshohocken PA, 2008.
[41] C.M. Hansson, B. Sorensen, The Threshold Concentration, The threshold concentration of chloride in concrete for the initiation of reinforcement corrosion, Corrosion Rates of Steel in Concrete, ASTM STP, Baltimore, Maryland, USA, 1990, p. 1065.
[42] N.J. Carino, Nondestructive techniques to investigate corrosion status in concrete structures, J. Perf. Constr. Fac. 13 (3) (1999) 96–107.
[43] ASTM C876, Standard Test Method for Half-Cell Potentials of Uncoated Reinforcing Steel in Concrete, ASTM International, West Conshohocken PA, 1991.
[44] H.W. Song, V. Saraswathy, Corrosion monitoring of reinforced concrete structures — a review, Int. J. Electrochem. Sci. 2 (2007) 1–28.
[45] Princeton Applied Research, Electrochemistry and corrosion overview and techniques, Application Note corr-4, http://new.ametek.com/contentmanager/files/PAR/088.pdf.
[46] M. Stern, A.L. Geary, Electrochemical polarisation: I. A theoretical analysis of the shape of polarisation curves, J. Electrochem. Soc. 104 (1) (1957) 56–63.
[47] ASTM G59 Test Method for Conducting Potentiodynamic Polarization Resistance Measurements, 2009.
[48] E. Ghali, Électrochimie, corrosion et protection, Département de mines et métallurgie, Cours GML 10443, Université Laval, Canada, Hiver, 2005.
[49] B. Assouli, Étude par émission acoustique associée aux méthodes électrochimiques de la corrosion et de la protection de l'alliage cuivre-zinc (60/40) en milieu neutre et alcalin, Thèse de doctorat, Université Ibn Toafail (Maroc) - INSA Lyon (France), Spécialité Génie des matériaux : Microstructure, comportement mécanique, durabilité, 2002,164p.
[50] N.S. Berke, M.C. Hicks, L. Li, M. Miltenberger, B. Miller, V. Munteanu, R. Carvajal, Accelerated mortar test method to determine chloride threshold values for corrosion initiation, in: N.S. Berke, M. Thomas, X. Yunping, L.L. Veleva (Eds.), Electrochemical Techniques for Evaluating Corrosion Performance and Estimating Service-life of Reinforced Concrete, ASTM STP 1457, ASTM International, West Conshohocken, PA, 2002.
[51] S.E. Hussain, A.S. Al-Gahtani, Resheeduzzafar, Chloride threshold for corrosion of reinforcement in concrete, ACI Mater. J. 93 (6) (1997) 534–538.
[52] T. Zhang, E. Samson, J. Marchand, Effect of temperature on ionic transport properties of concrete, Proceedings of the ConMAT Conference, August, Vancouver Canada, 2005.
[53] C. N. Chao, Étude sur l'hydratation des ciments composés CEM V - Application au comportement à long terme des bétons, Thèse de Doctorat, spécialité Chimie-Physique, Université de Bourgogne, 2007, 216p.
[54] F. Cassagnabère, M. Mouret, G. Escadeillas, Early hydration of clinker–slag–metakaolin combination in steam curing conditions, relation with mechanical properties, Cem. Concr. Res. 39 (2009) 1164–1173.
[55] J. Duchesne, M.A. Bérubé, The effectiveness of supplementary cementing materials in suppressing expansion due to ASR: another look at the reaction mechanisms. Part 1: concrete expansion and portlandite depletion, Cem. Concr. Res. 24 (1) (1994) 73–82.

[56] O. Oueslati, J. Duchesne, The effect of SCMs and curing time on resistance of mortars subjected to organic acids, Cem. Concr. Res. (2011), doi:10.1016/j.cemconres.2011.09.017.
[57] J.M. Khatib, S. Wild, Pore size distribution of metakaolin paste, Cem. Concr. Res. 26 (10) (1996) 1545–1553.
[58] C.L. Page, O. Vennesland, Pore solution composition and chloride binding capacity of silica-fume cement pastes, Mater. Constr. 16 (1983) 19–25.
[59] T.D. Marcotte, C.M. Hansson, The influence of silica fume on the corrosion resistance of steel in high performance concrete exposed to simulated sea water, J. Mat. Sci. 38 (2003) 4765–4776.